

**Fig. 5.** Miscoding specificities of the dI lesion in reactions catalyzed by pol  $\alpha$ , pol  $\eta$ , or pol  $\kappa\Delta C$ . Using unmodified and dI-modified 38-mer templates primed with an Alexa546-labeled 12-mer, we conducted primer extension reactions at 25 °C for 30 min in a buffer containing four dNTPs (100  $\mu$ M each) and either pol  $\alpha$  (200 fmol for unmodified and dI-modified templates), pol  $\kappa\Delta C$ , or pol  $\eta$  (20 fmol for unmodified and dI-modified templates), as described in Materials and Methods. The extended reaction products (>26 bases long) produced on the unmodified and dI-modified templates were extracted following PAGE. The recovered oligodeoxynucleotides were annealed to an unmodified 38-mer and cleaved with EcoRI restriction enzyme, as described in Materials and Methods. The entire product from the unmodified and dI-modified templates was subjected to two-phased PAGE (20 $\times$ 65 $\times$ 0.05 cm). Mobilities of reaction products were compared with those of 18-mer standards (Fig. 3) containing dC, dA, dG; or dT opposite the lesion and one-base ( $\Delta^1$ ) or two-base ( $\Delta^2$ ) deletions.

The mutation spectrum induced by  $\cdot$ NO has been investigated in a variety of experimental systems.  $\cdot$ NO gas showed mutagenicity in TK6 cells<sup>10</sup> and caused predominantly A:T $\rightarrow$ G:C transitions in plasmids replicated in cultured human and *E. coli* cells<sup>28,29</sup> and C $\rightarrow$ T transitions in a bacterial system.<sup>9</sup> Moreover,  $\cdot$ NO-releasing compounds exclusively resulted in G:C $\rightarrow$ A:T transitions in pSP189 plasmids propagated in human cells.<sup>30</sup> Using similar  $\cdot$ NO-releasing compounds, ONOO $^-$  caused G:C $\rightarrow$ T:A and G:C $\rightarrow$ C:G transversions with the same experimental system.<sup>31,32</sup> Thus, based on the information obtained from these previous reports, the mutation spectrum

by  $\cdot$ NO has not been extensively determined yet.<sup>33</sup> In our previous studies, the miscoding frequencies and specificities of dX, 8-NO $_2$ -dG, and 8-OxodG lesions were quantitatively determined by two-phased PAGE. As a result, 8-NO $_2$ -dG<sup>34</sup> and 8-OxodG<sup>17,35</sup> are miscoding lesions generating primarily G $\rightarrow$ T transversions (~20% and ~38%, respectively), while the miscoding spectrum of the dX adduct<sup>36</sup> exclusively shows G $\rightarrow$ A transitions (~50%), which differs from that of 8-NO $_2$ -dG and 8-OxodG. This indicates that each DNA adduct has a unique miscoding specificity and frequency. The mutation spectrum by  $\cdot$ NO can be hardly determined due to the presence of diverse

**Table 1.** Kinetic parameters for nucleotide insertion and chain extension reactions catalyzed by human DNA pol  $\alpha$ , pol  $\eta$ , and pol  $\kappa\Delta C$

	N:Z	Insertion dNTP			Extension dGTP			
		↓GAAGAAAGGAGA <sup>Alexa546</sup>			↓NGAAGAAAGGAGA <sup>Alexa546</sup>			
		5'CCTTCZCTTCITTCCTCCCTTT			5'CCTTCZCTTCITTCCTCCCTTT			
	$K_m$ ( $\mu$ M) <sup>a</sup>	$V_{max}$ (% min $^{-1}$ ) <sup>a</sup>	$F_{ins}$	$K_m$ ( $\mu$ M) <sup>a</sup>	$V_{max}$ (% min $^{-1}$ ) <sup>a</sup>	$F_{ext}$	$F_{ins} \times F_{ext}$	
Pol $\alpha$	T:A	0.56 $\pm$ 0.03	0.53 $\pm$ 0.02	1.0	0.41 $\pm$ 0.14	0.31 $\pm$ 0.03	1.0	1.0
	C:Z	0.73 $\pm$ 0.26	0.47 $\pm$ 0.03	0.718	0.48 $\pm$ 0.09	0.25 $\pm$ 0.01	0.679	0.487
	A:Z	N.D.	N.D.	N.D.	N.D.	N.D.	N.D.	N.D.
	G:Z	N.D.	N.D.	N.D.	N.D.	N.D.	N.D.	N.D.
Pol $\eta$	T:Z	9.74 $\pm$ 1.60	0.11 $\pm$ 0.07	1.21 $\times 10^{-2}$	7.09 $\pm$ 1.50	10.1 $\pm$ 0.65	1.92 $\times 10^{-2}$	2.32 $\times 10^{-4}$
	T:A	0.65 $\pm$ 0.17	5.37 $\pm$ 0.26	21.0	0.69 $\pm$ 0.13	7.49 $\pm$ 0.11	1.0	1.0
	C:Z	1.74 $\pm$ 0.58	7.79 $\pm$ 0.48	0.551	0.96 $\pm$ 0.18	8.44 $\pm$ 0.25	0.809	0.446
	A:Z	4.87 $\pm$ 1.22	1.28 $\pm$ 0.03	3.18 $\times 10^{-2}$	6.63 $\pm$ 0.76	2.66 $\pm$ 0.08	3.66 $\times 10^{-2}$	1.16 $\times 10^{-3}$
Pol $\kappa\Delta C$	G:Z	16.1 $\pm$ 1.03	1.00 $\pm$ 0.01	7.30 $\times 10^{-3}$	11.6 $\pm$ 4.23	1.14 $\pm$ 0.11	9.40 $\times 10^{-3}$	6.86 $\times 10^{-5}$
	T:Z	7.00 $\pm$ 1.97	1.19 $\pm$ 0.03	2.07 $\times 10^{-2}$	6.76 $\pm$ 0.41	4.99 $\pm$ 0.02	6.72 $\times 10^{-2}$	1.39 $\times 10^{-3}$
	T:A	1.43 $\pm$ 0.38	11.1 $\pm$ 0.47	1.0	0.55 $\pm$ 0.07	13.9 $\pm$ 0.54	1.0	1.0
	C:Z	1.36 $\pm$ 0.40	10.3 $\pm$ 0.44	0.987	0.79 $\pm$ 0.76	13.1 $\pm$ 0.12	0.651	0.642
	A:Z	15.5 $\pm$ 4.30	1.10 $\pm$ 0.05	9.23 $\times 10^{-3}$	10.7 $\pm$ 2.43	2.17 $\pm$ 0.07	8.13 $\times 10^{-3}$	7.50 $\times 10^{-5}$
	G:Z	84.0 $\pm$ 15.4	0.76 $\pm$ 0.30	1.12 $\times 10^{-3}$	12.8 $\pm$ 2.25	0.51 $\pm$ 0.05	1.57 $\times 10^{-3}$	1.75 $\times 10^{-6}$
	T:Z	23.5 $\pm$ 6.93	1.50 $\pm$ 0.11	8.26 $\times 10^{-3}$	5.28 $\pm$ 0.37	1.59 $\pm$ 0.03	1.18 $\times 10^{-2}$	9.74 $\times 10^{-5}$

Kinetics of nucleotide insertion and chain extension reactions were determined as described in Materials and Methods. Frequencies of nucleotide insertion ( $F_{ins}$ ) and chain extension ( $F_{ext}$ ) were estimated by the following equation:  $F = (V_{max}/K_m)_{[wrong\ pair]} / (V_{max}/K_m)_{[correct\ pair = dT:dA]}$ ; Z=dA or dI lesion.

N.D., not detectable.

<sup>a</sup> Data are expressed as mean $\pm$ SD obtained from three independent experiments.

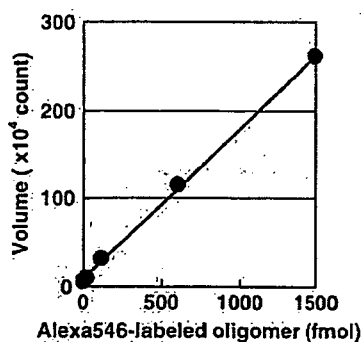


Fig. 6. Calibration curve using fluorescent oligomers labeled by Alexa546. Varying amounts of Alexa546-labeled oligomer were subjected to 20% denaturing PAGE. The volume of bands was quantitatively measured by using Molecular Imager FX Pro and Quantity One software (Bio-Rad) to find a linear range in the fluorescent analysis.

DNA adducts caused by <sup>17</sup>NO-involved species (Fig. 1) and its miscoding variety.<sup>17,34,35</sup> Therefore, the quantitative miscoding properties of each <sup>17</sup>NO-derived DNA adduct must be required to explore its roles in the inflammation-driven carcinogenesis.

The miscoding specificity of dI was determined by using an *in vitro* experimental system that can quantify base substitutions and deletions formed during replication in the presence of four dNTPs. Pol  $\alpha$ , pol  $\eta$ , and pol  $\kappa\Delta C$  incorporated dCMP (83.3%, 55.0%, and 74.7%, respectively) preferentially opposite the dI lesion rather than dTMP, the correct base (Fig. 5). Kamiya *et al.* reported earlier that mouse pol  $\alpha$  inserted dCMP and dTMP, the correct base, opposite the dI lesion.<sup>16</sup> In contrast, human pol  $\alpha$  promoted direct incorporation of dCMP only (Fig. 5). These indicate that the pols promote miscoding by incorporating dCMP opposite the dI lesion during DNA synthesis. Thus, dI is a highly miscoding lesion, generating A  $\rightarrow$  G transitions in human cells. Steady-state kinetic studies supported these results. When pol  $\alpha$ , pol  $\eta$ , and pol  $\kappa\Delta C$  were used,  $F_{ins} \times F_{ext}$  values for dC:dI pairs were 2100, 320, and 6600 times higher than those for dT:dI pairs, respectively (Table 1). Therefore, the kinetic results were consistent with that observed using two-phased PAGE analysis. Taken together, both analyses showed that human

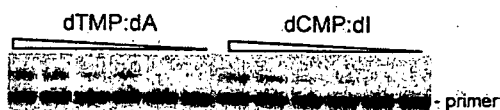


Fig. 7. Typical image of PAGE for kinetic studies performed by Alexa546 labeling. Using unmodified or dI-modified 38-mer templates (750 fmol) primed with an Alexa546-labeled 12-mer (500 fmol), we conducted primer extension reactions at 25 °C for 2 min in a buffer containing pol  $\kappa\Delta C$  (1 fmol) and either dTTP (0.25–25  $\mu$ M for unmodified templates) or dCTP (0.25–25  $\mu$ M for dI-modified templates), as described in Materials and Methods. The whole amount of the reaction mixture was subjected to 20% denaturing PAGE (30  $\times$  40  $\times$  0.05 cm).

DNA pols miscode at dI lesions by exclusively incorporating dCMP. The miscoding specificity was consistent with that observed in *E. coli*,<sup>9</sup> mammalian cells,<sup>10,37</sup> and mice exposed to <sup>17</sup>NO.<sup>15</sup>

To compare the relative bypass frequency of dI, dX, and 8-NO<sub>2</sub>-dG by pol  $\alpha$ , pol  $\eta$ , and pol  $\kappa\Delta C$ , these adducts were embedded in a similar sequence context<sup>34,36</sup> (Table 2). With pol  $\alpha$ , the  $F_{ins} \times F_{ext}$  ratio for the dC:dI/dT:dI pairs was 2100. This number was remarkably higher than that for the dT:dX/dC:dX (ratio=1.5) or dA:8-NO<sub>2</sub>-dG/dC:8-NO<sub>2</sub>-dG (ratio=0.01) pairs. Similar results were observed with pol  $\eta$  and pol  $\kappa\Delta C$ . The ratios of  $F_{ins} \times F_{ext}$  past dI were 2 orders of magnitude higher than those of dX and 8-NO<sub>2</sub>-dG. Thus, dI adducts promote a higher miscoding potential (A  $\rightarrow$  G transitions) than those of dX or 8-NO<sub>2</sub>-dG. However, the highly mutagenic dI lesions did not show serious mutation frequency<sup>9,10</sup> even though they were predominantly paired with the wrong base, dCMP. Endonuclease V (endo V) has shown to be a dI-specific endonuclease.<sup>38–40</sup> Methylpurine glycosylase also recognizes this lesion.<sup>41–43</sup> For instance, *E. coli* cells lacking the endo V (*nfi*) gene were shown to exhibit elevated mutation frequencies when exposed to nitrous acid. The increased mutations were predominantly A:T  $\rightarrow$  G:C mutations, followed by lesser G:C  $\rightarrow$  A:T mutations.<sup>44,45</sup> This indicates that endo V is primarily involved in the repair of dI lesions.<sup>44–48</sup>

The structure of double-stranded oligodeoxynucleotide containing the dI:dC pair was determined by thermodynamic and NMR studies.<sup>49,50</sup> dI can most stably pair with dC among four dNs, and its geometric structure is similar in form with the Watson-Crick structure (Fig. 8). dI has a carbonyl group at position C6 and a positive charge at position N1 after dA suffers from nitrosative deamination by <sup>17</sup>NO. Thus, since the structure of dI is similar to that of dG rather than dA, the dI adduct can predominantly pair with dC, the wrong base.

In conclusion, nonradioactive kinetic studies and two-phased PAGE were performed to explore the

Table 2.  $F_{ins} \times F_{ext}$  past DNA adducts by human DNA pol  $\alpha$ , pol  $\eta$ , and pol  $\kappa\Delta C$

	Z=	dI <sup>a</sup>	dX <sup>b</sup>	8-NO <sub>2</sub> -dG <sup>c</sup>
Pol $\alpha$	C:Z	<b>0.487</b>	$4.50 \times 10^{-3}$	$1.69 \times 10^{-3}$
	A:Z	N.D.	$2.18 \times 10^{-4}$	$1.31 \times 10^{-5}$
	G:Z	N.D.	$1.11 \times 10^{-5}$	$2.63 \times 10^{-6}$
	T:Z	$2.32 \times 10^{-4}$	$6.68 \times 10^{-3}$	$5.87 \times 10^{-6}$
Pol $\eta$	C:Z	<b>0.446</b>	$5.24 \times 10^{-2}$	$6.94 \times 10^{-3}$
	A:Z	$1.16 \times 10^{-3}$	$1.71 \times 10^{-3}$	$5.09 \times 10^{-3}$
	G:Z	$6.86 \times 10^{-5}$	$2.94 \times 10^{-4}$	$4.63 \times 10^{-4}$
	T:Z	$1.39 \times 10^{-3}$	<b>0.259</b>	$4.06 \times 10^{-4}$
Pol $\kappa\Delta C$	C:Z	<b>0.642</b>	$8.39 \times 10^{-3}$	$6.37 \times 10^{-5}$
	A:Z	$7.50 \times 10^{-5}$	$2.43 \times 10^{-6}$	$2.88 \times 10^{-5}$
	G:Z	$1.75 \times 10^{-6}$	$2.48 \times 10^{-6}$	$2.62 \times 10^{-6}$
	T:Z	$9.74 \times 10^{-5}$	$5.12 \times 10^{-2}$	$6.62 \times 10^{-7}$

Values in boldface show a primarily misincorporated base opposite the DNA adduct.

N.D., not detectable.

<sup>a</sup> Data were taken from Table 1.

<sup>b</sup> Data were taken from Ref. 36.

<sup>c</sup> Data were taken from Ref. 34.

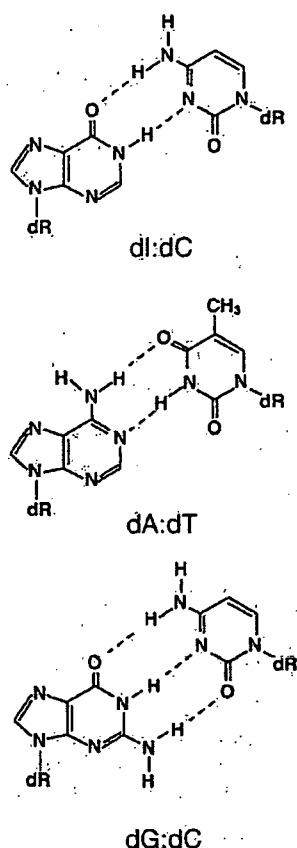


Fig. 8. Possible base pairing of the dI adduct with dC.

miscoding specificities and frequencies of the dI lesion catalyzed by Y-family human DNA pols. The dI adduct represents a highly miscoding lesion capable of generating A  $\rightarrow$  G transitions, indicating that this  $^{\circ}$ NO-induced lesion plays an important role in initiating inflammation-driven carcinogenesis.

## Materials and Methods

### General

Ultrapure dNTPs were from GE Healthcare. EcoRI restriction endonuclease (100 U/ $\mu$ L) was purchased from New England BioLabs. Blue Dextran (D5751) was obtained from Sigma. Human pol  $\alpha$  was obtained from CHIMERx (Milwaukee, WI). Human pol  $\eta$  was purified as previously described.<sup>19</sup> Human pol  $\kappa$  (pol  $\kappa\Delta$ C) was overexpressed in *E. coli* and purified as a C-terminally truncated form. The protein has 10 $\times$  His tag at the N-terminal position and contains 559 amino acids from the N-terminus (N. Niimi and T. Nohmi *et al.*, unpublished results).

### Preparation of oligodeoxynucleotides

All oligodeoxynucleotides, Alexa546 (Molecular Probes)-labeled primers, standard markers, and dI-modified template were obtained from Japan Bio Service Co. (Saitama,

Japan). Alexa546 was conjugated at the 5'-terminus of primers and standard markers. A single dI was located at the 20th position from the 5'-termini in the modified 38-mer template (5'-CATGCTGATGAATTCCTTCZCTTCTTTCCTCTCCCTTT, where Z is dI). The oligomers were purified by using 20% denaturing PAGE before use.

### Primer extension reactions

Primer extension reactions catalyzed by pol  $\alpha$ , pol  $\eta$ , or pol  $\kappa\Delta$ C were conducted at 25  $^{\circ}$ C for 30 min in a buffer (10  $\mu$ L) containing all four dNTPs (100  $\mu$ M each) using dI-modified and unmodified 38-mer templates (750 fmol) primed with an Alexa546-labeled 10-mer (500 fmol, 5'-AGAGGAAAGA) (Fig. 3). The reaction buffer for pol  $\alpha$  contains 40 mM Tris-HCl (pH 8.0), 5 mM MgCl<sub>2</sub>, 60 mM KCl, 10 mM dithiothreitol, 250  $\mu$ g/mL bovine serum albumin, and 2.5% glycerol. The reaction buffer for pol  $\eta$  and pol  $\kappa\Delta$ C contains 40 mM Tris-HCl (pH 8.0), 1 mM MgCl<sub>2</sub>, 10 mM dithiothreitol, 250  $\mu$ g/mL bovine serum albumin, 60 mM KCl, and 2.5% glycerol. Reaction was stopped by addition of 2  $\mu$ L formamide dye containing Blue Dextran (100 mg/mL) and ethylenediaminetetraacetic acid (50 mM) and incubation at 95  $^{\circ}$ C for 3 min. The whole amount of the reaction sample was subjected to 20% denaturing PAGE (30 $\times$ 40 $\times$ 0.05 cm). The positions of bands and homogeneities of oligodeoxynucleotides following PAGE were determined by using Molecular Imager FX Pro and Quantity One software (Bio-Rad). The linear range to quantitatively detect fluorescence-labeled oligomers was from 5 to 1500 fmol (Fig. 6).

### Quantitation of miscoding specificity

Using dI-modified and unmodified 38-mer oligodeoxynucleotide (750 fmol) primed with an Alexa546-labeled 12-mer (500 fmol, 5'-AGAGGAAAGAAG), we conducted primer extension reactions catalyzed by pol  $\alpha$  (200 fmol), pol  $\eta$  (20 fmol), or pol  $\kappa\Delta$ C (20 fmol) at 25  $^{\circ}$ C for 30 min in a buffer (10  $\mu$ L) containing all four dNTPs (100  $\mu$ M each) and subjected them to 20% denaturing PAGE (30 $\times$ 40 $\times$ 0.05 cm). Extended reaction products (>26 bases long) were extracted from the gel. The recovered oligodeoxynucleotides were annealed with an unmodified 38-mer, cleaved with EcoRI, and subjected to two-phased PAGE (20 $\times$ 65 $\times$ 0.05 cm) containing 7 M urea in the upper phase and no urea in the middle and bottom phases (each phase contains 18%, 20%, and 24% polyacrylamide, respectively). The phase width is approximately 10, 37, and 18 cm from the upper phase. To quantify base substitutions and deletions, we compared the mobility of the reaction products with those of Alexa546-labeled 18-mer standards containing dC, dA, dG, or dT opposite the lesion and one-base ( $\Delta^1$ ) or two-base ( $\Delta^2$ ) deletions<sup>17,18</sup> (Fig. 3).

### Steady-state kinetic studies of nucleotide insertion and extension

Kinetic parameters associated with nucleotide insertion opposite the dI lesion and chain extension from the 3' primer terminus were determined at 25  $^{\circ}$ C, using varying amounts of single dNTPs. For insertion kinetics, reaction mixtures containing dNTP (0–250  $\mu$ M) and either pol  $\alpha$  (20–200 fmol), pol  $\eta$  (2–20 fmol), or pol  $\kappa\Delta$ C (1–20 fmol) were incubated at 25  $^{\circ}$ C for 2 min in 10  $\mu$ L of Tris-HCl buffer (pH 8.0) using a 38-mer template (750 fmol) primed with an Alexa546-labeled 12-mer (500 fmol; 5'-AGAG-

GAAAGAAG). Reaction mixtures containing a 38-mer template (750 fmol) primed with an Alexa546-labeled 13-mer (500 fmol; 5'AGAGGAAAGAAGN, where N is C, A, G, or T), with varying amounts of dGTP (0–250  $\mu$ M) and either pol  $\alpha$  (20–200 fmol), pol  $\eta$  (1–20 fmol), or pol  $\kappa$   $\Delta$ C (1–20 fmol), were used to measure chain extension. The reaction samples were subjected to 20% denaturing PAGE (30 $\times$ 40 $\times$ 0.05 cm). The Michaelis constants ( $K_m$ ) and maximum rates of reaction ( $V_{max}$ ) were obtained from Hanes–Wolf plots. Frequencies of dNTP insertion ( $F_{ins}$ ) and chain extension ( $F_{ext}$ ) were determined relative to the dT:dA base pair according to the following equation:  $F = (V_{max}/K_m)_{[wrong\ pair]} / (V_{max}/K_m)_{[correct\ pair = dT:dA]}$ <sup>24,25</sup>

## Acknowledgements

This research was supported in part by Grants-in-aid for Scientific Research 19710059 from the Ministry of Education, Culture, Sports, Science and Technology (to M.Y.). This work was also partially supported by Health, Welfare, and Labor Science Research Grants (H18-food-general-009) and a Grant-in-aid (KHB1007) from the Japan Health Science Foundation (to M.H.).

## References

- Ohshima, H. & Bartsch, H. (1994). Chronic infections and inflammatory processes as cancer risk factors: possible role of nitric oxide in carcinogenesis. *Mutat. Res.* 305, 253–264.
- Cassell, G. H. (1998). Infectious causes of chronic inflammatory diseases and cancer. *Emerg. Infect. Dis.* 4, 475–487.
- Ohshima, H., Tatemichi, M. & Sawa, T. (2003). Chemical basis of inflammation-induced carcinogenesis. *Arch. Biochem. Biophys.* 417, 3–11.
- Burney, S., Caulfield, J. L., Niles, J. C., Wishnok, J. S. & Tannenbaum, S. R. (1999). The chemistry of DNA damage from nitric oxide and peroxy-nitrite. *Mutat. Res.* 424, 37–49.
- deRojas-Walker, T., Tamir, S., Ji, H., Wishnok, J. S. & Tannenbaum, S. R. (1995). Nitric oxide induces oxidative damage in addition to deamination in macrophage DNA. *Chem. Res. Toxicol.* 8, 473–477.
- Yermilov, V., Rubio, J., Becchi, M., Friesen, M. D., Pignatelli, B. & Ohshima, H. (1995). Formation of 8-nitroguanine by the reaction of guanine with peroxy-nitrite *in vitro*. *Carcinogenesis*, 16, 2045–2050.
- Yermilov, V., Rubio, J. & Ohshima, H. (1995). Formation of 8-nitroguanine in DNA treated with peroxy-nitrite *in vitro* and its rapid removal from DNA by depurination. *FEBS Lett.* 376, 207–210.
- Lewis, R. S., Tannenbaum, S. R. & Deen, W. M. (1995). Kinetics of N-nitrosation in oxygenated nitric oxide solutions at physiological pH: role of nitrous anhydride and effects of phosphate and chloride. *J. Am. Chem. Soc.* 117, 3933–3939.
- Wink, D. A., Kasprzak, K. S., Maragos, C. M., Elespuru, R. K., Misra, M., Dunams, T. M. *et al.* (1991). DNA deaminating ability and genotoxicity of nitric oxide and its progenitors. *Science*, 254, 1001–1003.
- Nguyen, T., Brunson, D., Crespi, C. L., Penman, B. W., Wishnok, J. S. & Tannenbaum, S. R. (1992). DNA damage and mutation in human cells exposed to nitric oxide *in vitro*. *Proc. Natl Acad. Sci. USA*, 89, 3030–3034.
- Caulfield, J. L., Wishnok, J. S. & Tannenbaum, S. R. (1998). Nitric oxide-induced deamination of cytosine and guanine in deoxynucleosides and oligonucleotides. *J. Biol. Chem.* 273, 12689–12695.
- Dong, M., Wang, C., Deen, W. M. & Dedon, P. C. (2003). Absence of 2'-deoxyoxanosine and presence of abasic sites in DNA exposed to nitric oxide at controlled physiological concentrations. *Chem. Res. Toxicol.* 16, 1044–1055.
- Pang, B., Zhou, X., Yu, H., Dong, M., Taghizadeh, K., Wishnok, J. S. *et al.* (2007). Lipid peroxidation dominates the chemistry of DNA adduct formation in a mouse model of inflammation. *Carcinogenesis*, 28, 1807–1813.
- Dong, M. & Dedon, P. C. (2006). Relatively small increases in the steady-state levels of nucleobase deamination products in DNA from human TK6 cells exposed to toxic levels of nitric oxide. *Chem. Res. Toxicol.* 19, 50–57.
- Gal, A. & Wogan, G. N. (1996). Mutagenesis associated with nitric oxide production in transgenic SJL mice. *Proc. Natl Acad. Sci. USA*, 93, 15102–15107.
- Kamiya, H., Sakaguchi, T., Murata, N., Fujimuro, M., Miura, H., Ishikawa, H. *et al.* (1992). *In vitro* replication study of modified bases in ras sequences. *Chem. Pharm. Bull.* 40, 2792–2795.
- Masutani, C., Araki, M., Yamada, A., Kusumoto, R., Nogimori, T., Maekawa, T. *et al.* (1999). Xeroderma pigmentosum variant (XP-V) correcting protein from HeLa cells has a thymine dimer bypass DNA polymerase activity. *EMBO J.* 18, 3491–3501.
- Ogi, T., Kato, T., Jr, Kato, T. & Ohmori, H. (1999). Mutation enhancement by DINB1, a mammalian homologue of the *Escherichia coli* mutagenesis protein dinB. *Genes Cells*, 4, 607–618.
- Gerlach, V. L., Aravind, L., Gotway, G., Schultz, R. A., Koonin, E. V. & Friedberg, E. C. (1999). Human and mouse homologs of *Escherichia coli* DinB (DNA polymerase IV), members of the UmuC/DinB superfamily. *Proc. Natl Acad. Sci. USA*, 96, 11922–11927.
- Goodman, M. F. & Tippen, B. (2000). The expanding polymerase universe. *Nat. Rev., Mol. Cell Biol.* 1, 101–109.
- Kunkel, T. A., Pavlov, Y. L. & Bebenek, K. (2003). Functions of human DNA polymerases  $\eta$ ,  $\kappa$  and  $\iota$  suggested by their properties, including fidelity with undamaged DNA templates. *DNA Repair*, 3, 135–149.
- Shibutani, S. (1993). Quantitation of base substitutions and deletions induced by chemical mutagens during DNA synthesis *in vitro*. *Chem. Res. Toxicol.* 6, 625–629.
- Shibutani, S., Suzuki, N., Matsumoto, Y. & Grollman, A. P. (1996). Miscoding properties of 3,N<sup>4</sup>-etheno-2'-deoxycytidine in reactions catalyzed by mammalian DNA polymerases. *Biochemistry*, 35, 14992–14998.
- Mendelman, L. V., Boosalis, M. S., Petruska, J. & Goodman, M. F. (1989). Nearest neighbor influences on DNA polymerase insertion fidelity. *J. Biol. Chem.* 264, 14415–14423.
- Mendelman, L. V., Petruska, J. & Goodman, M. F. (1990). Base mispair extension kinetics. Comparison of DNA polymerase alpha and reverse transcriptase. *J. Biol. Chem.* 265, 2338–2346.
- Clark, J. M., Joyce, C. M. & Beardsley, G. P. (1987). Novel blunt-end addition reactions catalyzed by DNA polymerase I of *Escherichia coli*. *J. Mol. Biol.* 198, 123–127.

27. Terashima, I., Suzuki, N., Dasaradhi, L., Tan, C.-K., Downey, K. M. & Shibutani, S. (1998). Translesional synthesis on DNA templates containing an estrogen quinone derived adduct: N<sup>2</sup>-(2-hydroxyestron-6-yl)-2'-deoxyguanosine and N<sup>6</sup>-(2-hydroxyestron-6-yl)-2'-deoxyadenosine. *Biochemistry*, **37**, 13807-13815.
28. Routledge, M. N., Wink, D. A., Keefer, L. K. & Dipple, A. (1993). Mutations induced by saturated aqueous nitric oxide in the pSP189 *supF* gene in human Ad293 and *E. coli* MBM7070 cells. *Carcinogenesis*, **14**, 1251-1254.
29. Kelman, D. J., Christodolou, D., Wink, D. A., Keefer, L. K., Srinivasan, A. & Dipple, A. (1997). Relative mutagenicities of gaseous nitrogen oxides in the *supF* gene of pSP189. *Carcinogenesis*, **18**, 1045-1048.
30. Routledge, M. N., Wink, D. A., Keefer, L. K. & Dipple, A. (1994). DNA sequence changes induced by two nitric oxide donor drugs in the *supF* assay. *Chem. Res. Toxicol.* **7**, 628-632.
31. Juedes, M. J. & Wogan, G. N. (1996). Peroxynitrite-induced mutation spectra of pSP189 following replication in bacteria and in human cells. *Mutat. Res.* **349**, 51-61.
32. Kim, M. Y., Dong, M., Dedon, P. C. & Wogan, G. N. (2005). Effects of peroxynitrite dose and dose rate on DNA damage and mutation in the *supF* shuttle vector. *Chem. Res. Toxicol.* **18**, 76-86.
33. Routledge, M. N. (2000). Mutations induced by reactive nitrogen oxide species in the *supF* forward mutation assay. *Mutat. Res.* **450**, 95-105.
34. Suzuki, N., Yasui, M., Geacintov, N. E., Shafirovich, V. & Shibutani, S. (2005). Miscoding events during DNA synthesis past the nitration-damaged base 8-nitroguanine. *Biochemistry*, **44**, 9238-9245.
35. Shibutani, S., Takeshita, M. & Grollman, A. P. (1991). Insertion of specific bases during DNA synthesis past the oxidation-damaged base 8-oxodG. *Nature*, **349**, 431-434.
36. Yasui, M., Suzuki, N., Miller, H., Matsuda, T., Matsui, S. & Shibutani, S. (2004). Translesion synthesis past 2'-deoxyxanthosine, a nitric oxide-derived DNA adduct, by mammalian DNA polymerases. *J. Mol. Biol.* **344**, 665-674.
37. Kamiya, H., Miura, H., Kato, H., Nishimura, S. & Ohtsuka, E. (1992). Induction of mutation of a synthetic c-Ha-ras gene containing hypoxanthine. *Cancer Res.* **52**, 1836-1839.
38. Yao, M. & Kow, Y. W. (1996). Cleavage of insertion/deletion mismatches, flap and pseudo-Y DNA structures by deoxyinosine 3'-endonuclease from *Escherichia coli*. *J. Biol. Chem.* **271**, 30672-30676.
39. Yao, M., Hatahet, Z., Melamed, R. J. & Kow, Y. W. (1994). Purification and characterization of a novel deoxyinosine-specific enzyme, deoxyinosine 3' endonuclease, from *Escherichia coli*. *J. Biol. Chem.* **269**, 16260-16268.
40. Yao, M. & Kow, Y. W. (1995). Interaction of deoxyinosine 3'-endonuclease from *Escherichia coli* with DNA containing deoxyinosine. *J. Biol. Chem.* **270**, 28609-28616.
41. Saparbaev, M. & Laval, J. (1994). Excision of hypoxanthine from DNA containing dIMP residues by the *Escherichia coli*, yeast, rat, and human alkylpurine DNA glycosylases. *Proc. Natl. Acad. Sci. USA*, **91**, 5873-5877.
42. Fortini, P., Parlanti, E., Sidorkina, O. M., Laval, J. & Dogliotti, E. (1999). The type of DNA glycosylase determines the base excision repair pathway in mammalian cells. *J. Biol. Chem.* **274**, 15230-15236.
43. Miao, F., Bouziane, M. & O'Connor, T. R. (1998). Interaction of the recombinant human methylpurine-DNA glycosylase (MPG protein) with oligodeoxyribonucleotides containing either hypoxanthine or abasic sites. *Nucleic Acids Res.* **26**, 4034-4041.
44. Schouten, K. A. & Weiss, B. (1999). Endonuclease V protects *Escherichia coli* against specific mutations caused by nitrous acid. *Mutat. Res.* **435**, 245-254.
45. Weiss, B. (2006). Evidence for mutagenesis by nitric oxide during nitrate metabolism in *Escherichia coli*. *J. Bacteriol.* **188**, 829-833.
46. Guo, G. & Weiss, B. (1998). Endonuclease V (*nfi*) mutant of *Escherichia coli* K-12. *J. Bacteriol.* **180**, 46-51.
47. Dong, M., Vongchampa, V., Gingipalli, L., Cloutier, J. F., Kow, Y. W., O'Connor, T. & Dedon, P. C. (2006). Development of enzymatic probes of oxidative and nitrosative DNA damage caused by reactive nitrogen species. *Mutat. Res.* **594**, 120-134.
48. Weiss, B. (2001). Endonuclease V of *Escherichia coli* prevents mutations from nitrosative deamination during nitrate/nitrite respiration. *Mutat. Res.* **461**, 301-309.
49. Kawase, Y., Iwai, S., Inoue, H., Miura, K. & Ohtsuka, E. (1986). Studies on nucleic acid interactions. I. Stabilities of mini-duplexes (dG2A4XA4G2-dC2T4YT4C2) and self-complementary d(GGGAAXYTTCCC) containing deoxyinosine and other mismatched bases. *Nucleic Acids Res.* **14**, 7727-7736.
50. Uesugi, S., Oda, Y., Ikehara, M., Kawase, Y. & Ohtsuka, E. (1987). Identification of I:A mismatch base-pairing structure in DNA. *J. Biol. Chem.* **262**, 6965-6968.